Published in final edited form as:
J Control Release. 2010 January 25; 141(2): 137–144. doi:10.1016/j.jconrel.2009.09.004.

Nanoparticle-mediated combination chemotherapy and photodynamic therapy overcomes tumor drug resistance

Ayman Khdair[a,b], **Di Chen**[c], **Yogesh Patil**[a,d], **Linan Ma**[e], **Q. Ping Dou**[c], **Malathy P.V. Shekhar**[f,g], and **Jayanth Panyam**[d,e,*]

[a]Department of Pharmaceutical Sciences, Eugene Applebaum College of Pharmacy and Health Sciences, Wayne State University, Detroit, MI 48201, United States

[b]Department of Pharmaceutical Sciences and Pharmaceutics, Applied Science University, Amman 11931, Jordan

[c]Population Studies Program, Karmanos Cancer Institute, Detroit, MI 48201, United States

[d]Department of Pharmaceutics, University of Minnesota, Minneapolis, MN 55455, United States

[e]Masonic Cancer Center, Minneapolis, MN 55455, United States

[f]Breast Cancer Program, Karmanos Cancer Institute, Detroit, MI 48201, United States

[g]Department of Pathology, Wayne State University School of Medicine, Detroit, MI 48201, United States

Abstract

Tumor drug resistance significantly limits the success of chemotherapy in the clinic. Tumor cells utilize multiple mechanisms to prevent the accumulation of anticancer drugs at their intracellular site of action. In this study, we investigated the anticancer efficacy of doxorubicin in combination with photodynamic therapy using methylene blue in a drug-resistant mouse tumor model. Surfactant-polymer hybrid nanoparticles formulated using an anionic surfactant, Aerosol-OT™ (AOT), and a naturally occurring polysaccharide polymer, sodium alginate, were used for synchronized delivery of the two drugs. Balb/c mice bearing syngeneic JC tumors (mammary adenocarcinoma) were used as a drug-resistant tumor model. Nanoparticle-mediated combination therapy significantly inhibited tumor growth and improved animal survival. Nanoparticle-mediated combination treatment resulted in enhanced tumor accumulation of both doxorubicin and methylene blue, significant inhibition of tumor cell proliferation, and increased induction of apoptosis. These data suggest that nanoparticle-mediated combination chemotherapy and photodynamic therapy using doxorubicin and methylene blue has significant therapeutic potential against drug-resistant tumors.

Keywords

Chemotherapy; Nanoparticles; Photosensitizer; Drug efflux; Drug resistance; Reactive oxygen species

[*]Corresponding author. Department of Pharmaceutics, College of Pharmacy, 308 Harvard St. SE., Minneapolis, MN 55455, United States. Tel.: +1 612 624 0951; fax: +1 612 626 2125. jpanyam@umn.edu (J. Panyam).

1. Introduction

Development of drug resistance significantly limits the success of chemotherapy in cancer patients and contributes to cancer recurrence and high mortality rates [1]. Tumor cells utilize specific mechanisms to survive toxic concentrations of anticancer agents. Overexpression of key proteins such as Bcl-2 and Mdm2 [2], Hsp70 [3], and mutations in *TP53* [4] have been correlated to drug resistance. In addition, overexpression of drug efflux transporters like P-glycoprotein (P-gp) [5] and sequestration of drug in acidic intracellular organelles [6] or in the acidic tumor microenvironment [7] reduce availability of the drug at its site of action inside the tumor cell. The multi-factorial nature of drug resistance warrants therapies that employ multiple mechanisms to kill the tumor cell.

Photodynamic therapy (PDT) is based on the concept that photosensitizers, when exposed to light of specific wavelength, generate cytotoxic reactive oxygen species (ROS) capable of killing tumor cells [8]. In addition to their photodynamic properties, photosensitizers like methylene blue also inhibit P-gp-mediated efflux of anticancer drugs [9]. At the cellular level, this results in increased availability of the anticancer drug at its site of action. PDT has also been shown to damage tumor vasculature through direct effects on vascular endothelial cells [10]. Another important advantage of combining PDT with chemotherapy is the potential for inducing antitumor immunity [11]. Based on these multiple mechanisms, we rationalized that methylene blue-mediated PDT could significantly enhance the cytotoxicity of drugs like doxorubicin in drug-refractory cancers.

A major issue with chemotherapy and PDT is the decreased therapeutic efficacy and increased toxicity associated with the non-specific accumulation of therapeutic agents in non-target tissues. For example, doxorubicin causes cardiotoxicity due its accumulation in the heart [12]. Similarly, clinical use of methylene blue in PDT has been limited because of its extensive accumulation and inactivation in erythrocytes and endothelial cells [13,14]. Encapsulation in a carrier like nanoparticles can significantly improve the accumulation of the therapeutic agent in the target tumor tissue through ‘Enhanced Permeation and Retention’ effect [15]. Further, encapsulation in nanoparticles can protect the drugs from inactivation in the biological environment [16,17]. We have recently reported the fabrication of a novel surfactant-polymer nanoparticle delivery system suitable for efficient cellular delivery of charged, polar drugs like methylene blue and doxorubicin [18,19]. These nanoparticles are fabricated from an anionic surfactant, Aerosol-OT™ (AOT), a pharmaceutical excipient [20], and a naturally occurring polysaccharide polymer, sodium alginate [21]. Our previous studies show that, in addition to improving the cellular delivery of encapsulated drugs, AOT-alginate nanoparticles significantly improve the ROS yield of photosensitizers like methylene blue [22]. In the current study, using AOT-alginate nanoparticles as a carrier, we investigated the efficacy of combination PDT and chemotherapy in a mouse drug-resistant mammary adenocarcinoma tumor model, and demonstrated that combining PDT with chemotherapy could overcome drug resistance by invoking multiple anticancer mechanisms.

2. Materials and methods

2.1. Materials

Methylene blue, doxorubicin, ammonium acetate, sodium alginate, polyvinyl alcohol, and calcium chloride were purchased from Sigma-Aldrich (St. Louis, MO). AOT, acetonitrile, methanol, methylene chloride, and sodium acetate were purchased from Fisher Scientific (Chicago, IL). RPMI 1640 cell culture medium and phosphate buffered saline (PBS) were purchased from Invitrogen (Carlsbad, CA). JC tumor cells were purchased from American Type Culture Collection (Manassas, VA).

2.2. Methods

2.2.1. Nanoparticle formulation and characterization—Nanoparticles loaded with doxorubicin, methylene blue, or both drugs were formulated using multiple emulsification cross-linking technique [18]. In brief, 1 ml of aqueous solution of sodium alginate (1% w/v) containing methylene blue (5 mg) and doxorubicin (5 mg) was emulsified into 2 ml of 2.5% w/v AOT solution in methylene chloride by sonication for 1 min over an ice bath (Sonicator 3000™, Misonix, Farmingdale, NY). The water-in-oil emulsion was further emulsified into 15 ml of aqueous polyvinyl alcohol solution (2% w/v) to form a water-in-oil-in-water double emulsion. Following this, the emulsion was stirred using a magnetic stirrer, and 5 ml of aqueous calcium chloride (60% w/v) was gradually added. The emulsion was further stirred for 18 h at ambient conditions and then under vacuum for 1 h to completely evaporate methylene chloride. This procedure results in nanoparticles with less than 10 ppm methylene chloride [18]. To remove free doxorubicin and methylene blue and excess polyvinyl alcohol, nanoparticles suspension was subjected to ultracentrifugation (145,000×*g* for 30 min, Beckman, Palo Alta, CA) thrice and washed in between with deionized water. To separate nanoparticles from aggregates, suspension was then centrifuged for 3 min at 1000 rpm (Eppendorf® 5810 R, Eppendorf, Westbury, NY). Dry nanoparticles were obtained by freeze-drying (FreeZone 4.5®, Labconco, Kansas City, MO) of the supernatant after the final centrifugation step. Nanoparticles were characterized for morphology and size by atomic force microscopy (AFM) in the tapping mode using silicon tapping tips (TESP, VEECO) of nominal radius less than 10 nm as described previously [18]. Nano-particles suspended in water (100 μg/ml) were spread over a thin layer of polyethyleneimine-coated glass coverslip and then air dried. Nanoscope III (Digital Instruments/VEECO) with an E scanner (maximum scan area=14.2×14.2 μm^2) was used to measure particle size. One Hz scan rate and ~0.4 integral gain and ~0.7 proportional gain were used. Diameters of at least 50 particles in 10 different fields were measured and the numerical average was calculated. Particle size was confirmed using dynamic light scattering (90Plus®, Brookhaven Instruments, Holtsville, NY). Nanoparticle suspension in deionized water (50 μg/ml) was sonicated and then subjected to particle size measurement and analyzed using non-negatively constrained least square algorithm. Surface charge of nanoparticles was determined by using electrophoretic light scattering. About 1 mg of nanoparticles was suspended in 1 ml deionized water by sonication and then zeta potential was determined using a zeta potential analyzer (90Plus®).

Amount of methylene blue and doxorubicin loaded in nanoparticles was determined using HPLC. About 5 mg of nanoparticles was extracted for 2 h in the dark with 10 ml methanol and then centrifuged for 10 min at 13,000 rpm. The supernatant was injected into a Beckman Coulter System Gold® HPLC (Fullerton, CA) supplied with 125 solvent module and 508 auto-injector. Synergi™ Polar-RP column (4.6×150 mm ODS and 4 μ particle size, Phenomenex, Torrance, CA), UV detection at 598 nm (168 PDA UV/Vis detector, Beckman) and fluorescence detection (FP-2020 *plus* fluorescence detector; JASCO, Easton, MD) at 505/550 nm ex/em wavelengths were used. Mobile phase consisting of acetonitrile and ammonium acetate (10 mM; adjusted to pH 3.5 with glacial acetic acid) in (78:22) ratio at a flow rate of 1 ml/min was used. Retention time was ~4.5 and ~9.5 min for doxorubicin and methylene blue, respectively. Drug loading in nanoparticles was defined as the amount (mg) of methylene blue or doxorubicin in 100 mg of nanoparticles.

2.2.2. Mouse tumor model—All studies involving animals in this report were performed according to the guidelines of the Animal Investigation Committee of Wayne State University. Female Balb/c mice (Charles River Laboratories, Wilmington, MA), 4–6 weeks old, were injected subcutaneously in the right hindquarter with 1×10^6 JC cells suspended in serum-free RPMI 1640 medium. The JC cell line was chosen for the studies due to its

spontaneous derivation, *in vitro* expression of the P-gp-mediated drug-resistant phenotype, and reproducible *in vivo* growth [23].

2.2.3. Treatment administration—Mice that developed tumors of about 100 mm^3 were randomized into 7 treatment groups. Animals were injected with 0.1 ml of PBS containing free or nanoparticle-encapsulated doxorubicin and methylene blue (4 mg and 8 mg/kg, respectively) via a lateral tail vein. Some groups received nanoparticles loaded with only methylene blue or only doxorubicin. Animals that received PBS (vehicle) or blank nanoparticles in PBS were used as controls. About 24 h after treatment, animals were anesthetized and covered with aluminum foil, leaving the tumor exposed. Tumors were irradiated with 50 J/cm^2 dose of non-coherent light at 665 nm (LumaCare™ LC-122, Newport Beach, CA). This dose of light was chosen based on previously published studies [24]. Mice treated with the nanoparticles encapsulating doxorubicin and methylene blue as above but without light exposure were used as dark controls. All the treatments were administered only once. Tumor volumes were measured every third day for 30 days using a digital caliper. Survival data was analyzed based on when the animal died because of the tumor burden or had to be sacrificed when the tumor volume reached a pre-set target (2000 mm^3).

2.2.4. Immunohistochemistry studies—Tumors were induced and animals were treated as described above. Tumor tissues excised at the end of the study (day 30 or 2000 cm^3 tumor volume) were fixed in buffered formalin and then paraffin-embedded. After deparaffinization, sections were stained with antibodies against proliferating cell nuclear antigen (PCNA, Dako North America, Inc., Carpentaria, CA) or CD34 (Cell Sciences, Canton, MA). Positive staining was detected with appropriate biotinylated secondary antibody followed by incubation with streptavidin-horseradish peroxidase, and development with 3-amino-9-ethylene carbazol (DAKO). Sections were counterstained with hematoxylin. Microvessel density was determined in a blinded fashion by light microscopy. Areas of most intense neovascularization were identified by scanning tumor sections at low power (20×) and counted at high power magnification (400×). At least five separate fields were counted. Presence of apoptosis was detected with the terminal deoxynucleotidyl transferase-mediated nick-end-labeling assay (TUNEL; ApopTag® Peroxidase In Situ Apoptosis Detection Kit, Chemicon-Millipore Company, Billerica, MA) according to manufacturer's recommended procedure. Cells that stained positive for TUNEL or PCNA were counted at 400× magnification in at least 5 different fields (N1000 cells). Images of stained sections were acquired using a light microscope (Axiovert 40CFL microscope; Carl Zeiss MicroImaging, Inc., Thornwood, NY) equipped with a digital camera (ProGres® C3, JENOPIK Laser, Jena, Germany).

2.2.5. Tumor accumulation studies—Animals that developed tumors of about 100 mm^3 were injected with 0.1 ml of PBS containing free or nanoparticle-encapsulated doxorubicin and methylene blue (4 mg and 8 mg/kg, respectively) as described above. At 3 h post-injection, animals were euthanized and tumors along with heart, lung, kidney, brain, spleen, liver, and blood were collected. Collected organs were homogenized in 2 ml deionized water using a tissue homogenizer (Tissuemiser, Fisher Scientific, Chicago, IL) and then further homogenized after the addition of 100 ng verapamil (internal standard). Tissue homogenates were then lyophilized (FreeZone 4.5®, Labconco, Kansas City, MO). Dry tissues were weighed and extracted with 5 ml of methanol/chloroform mixture (65:35) using a shaker (Labquake™shaker, Barnstead Thermolyne, Dubuque, IA) for 5 h in dark at room temperature. The extract was centrifuged for 10 min at 4°C and 13,000 rpm. Supernatant was evaporated under nitrogen gas (N-EVAP™; Organomation Associates, Inc., Berlin, MA). Residues were then reconstituted in 100 μl of a 78:22 mixture of acetonitrile

and ammonium acetate (10 mM; adjusted to pH 3.2with glacial acetic acid) and centrifuged for 20 min at 20,000×*g*. Doxorubicin and methylene blue concentrations in the supernatant were analyzed using LC-MS/MS. A mobile phase gradient from 84% to 40% acetonitrile in ammonium acetate buffer (10 mM, pH 3.2) over 23 min at a flow rate of 13 μl/min was used. An Agilent® 1100 series capillary HPLC system (Agilent Technologies, Palo Alto, California) was used for chromatographic separation. A Finnigan TSQ® Quantum Ultra AM triple quadrupole mass spectrometer (Thermo Electron, San Jose, California) operated in the positive ion mode was used for mass spectroscopy. The samples (8 μl) were injected into Synergi™ Hydro-RP® capillary column (0.3×250 mm and 4 μm; Phenomenex, Torrance, CA). Doxorubicin (precursor-to-product *m/z* 544→397), verapamil (precursor-to-product *m/z* 455→165) and methylene blue (precursor-to-product *m/z* 284→268) were eluted at ~3, 5 and 8 min, respectively. Doxorubicin and methylene blue amounts were normalized to the dry tissue weight.

2.2.6. Statistical analyses

One-way ANOVA was used to analyze differences in TUNEL, CD34 and PCNA-positive cells among treatment groups. Generalized linear mixed effect ANOVA (mixed model) following natural log transformation of tumor volumes was used to analyze tumor growth inhibition data. The differences in the slopes of tumor growth curves were tested by Bonferroni adjustment. Differences in survival rate in treatment groups were analyzed by Kaplan–Meier survival analysis. A probaility level of $p<0.05$ was considered significant.

3. Results

3.1. Nanoparticle characterization

AFM studies indicated that nanoparticles loaded with both doxoru-bicin and methylene blue had a near spherical morphology (Fig. 1), with a number-average lateral diameter of 40±7 nm. Dynamic light scattering (DLS) studies showed that nanoparticles had a number-average diameter ~73 nm. The difference in particle size measurement between AFM and DLS studies could be attributed to the fact that DLS measures diameter of hydrated particles while AFM measures the size of dry particles. Zeta potential measurements showed that drug-loaded nanoparticles had a net surface charge of −24.6±1.1 mV. Methylene blue and doxorubicin were efficiently encapsulated in nanoparticles with an average loading of 13.0±0.6% w/w (82% encapsulation efficiency) and 6.9±0.1% w/w (78% encapsulation efficiency), respectively.

3.2. Tumor growth inhibition with combination therapy

The tumor growth in animals that received the combination of two drugs in nanoparticles with PDT was significantly slower than that in animals that received other treatments (Fig. 2A; $p<0.05$). The mean tumor volume in the methylene blue–doxorubicin nanoparticle–PDT group was 58% lower than that in the group that received the vehicle at the end of the study. Mice treated with doxorubicin and methylene blue in nanoparticles without light exposure (dark control) also resulted in slower tumor growth compared to vehicle-treated control; however, the % inhibition was less than that observed in the group that received the light exposure. Treatment with methylene blue nanoparticles and light (no doxorubicin) resulted in marginal inhibition of tumor growth compared to vehicle-treated control. Treatment with equivalent doses of free doxorubicin and methylene blue along with light exposure did not result in significant inhibition of tumor growth. Similarly, blank nanoparticles had no effect on tumor growth. Other controls (free doxorubicin, free methylene blue, and methylene blue nanoparticles in the absence of light) were not investigated because our preliminary studies demonstrated that these treatments have no effect on tumor cell viability [25].

Survival of animals closely followed the tumor growth profile. Mice treated with methylene blue–doxorubicin nanoparticles and light exposure survived longer compared to those that received other treatments ($p<0.05$; Fig. 2B). Treatment with methylene blue–doxorubicin in nanoparticles without light exposure also resulted in improved animal survival compared to those treated with vehicle or blank nanoparticles.

3.3. Inhibition of cellular proliferation

As can be seen in Fig. 3, treatment with nanoparticle-encapsulated methylene blue and doxorubicin along with light resulted in fewer PCNA-positive cells (5±2%) compared to control groups ($p<0.05$). Tumors from vehicle or blank nanoparticle-treated mice demonstrated 37±9% and 31±2% $PCNA^+$ cells, respectively. Treatment with doxorubicin nanoparticles (27±5%) or free methylene blue and doxorubicin combination with light (27±3%) had no effect on tumor cell proliferation. Treatment with combination nanoparticles without light exposure resulted in a slight decrease in $PCNA^+$ cells (17±5%). Tumors treated with methylene blue nanoparticles along with light exposure also demonstrated significantly reduced $PCNA^+$ cells (7±1%, $p<0.05$).

3.4. Induction of apoptosis

In order to determine whether induction of apoptosis contributed to tumor growth inhibition, tumor tissues were subjected to TUNEL assay. As can be seen from images in Fig. 4, tumors that received nanoparticle-encapsulated methylene blue and doxorubicin along with light exposure had significantly higher fraction of apoptotic cells (15±5%) than those that received the doxorubicin nanoparticle treatment (4±2%, $p<0.05$). Dark control group (mice treated with nanoparticle-encapsulated doxorubicin and methylene blue without light exposure) also showed slightly increased apoptosis (8±2%). Treatment with methylene blue nanoparticles along with light exposure resulted in 6±2% apoptotic cells. However, treatment with combination of free doxorubicin and methylene blue along with light exposure resulted in only ~1% $TUNEL^+$ cells, which was comparable to that with vehicle and blank nanoparticle treatments.

3.5. Tumor microvessel damage

Immunohistochemical staining with anti-CD34 antibody was performed to determine whether neovasculature of tumors was affected by treatment regimens. Although the number of CD34+ microvessels was not statistically different for the different groups, the microvessels in tumors that received nanoparticle-encapsulated methylene blue and doxorubicin along with light exposure were faint, diffuse and deformed (shown by arrows in Fig. 5) as compared to those in the other groups that were darkly stained and appeared to be intact.

3.6. Tumor accumulation studies

To determine the effect of encapsulation in nanoparticles on tumor accumulation of doxorubicin and methylene blue, distribution of the two drugs in different organs and tumor tissue was determined 3 h post administration. Encapsulation in nanoparticles resulted in a significant increase in the amount of doxorubicin and methylene blue delivered to the target tumor tissue (~4-fold increase for doxorubicin and a 3-fold increase for methylene blue, Fig. 6). Although not statistically significant, nanoparticles resulted in lower accumulation of doxorubicin in the heart. In addition, encapsulation in nanoparticles resulted in a ~10-fold reduction in the blood level of methylene blue.

4. Discussion

Clinical efficacy of many anticancer drugs is limited by the development of drug resistance [26]. Distribution of the drug to non-target tissues, reduced drug accumulation in the tumor tissue, and poor penetration of the drug into the tumor cell contribute to reduced anticancer efficacy. In our studies, doxorubicin, either free or encapsulated in nanoparticles, was not effective against JC tumors. This is in agreement with previous studies, which have shown that JC tumor cells overexpress P-gp, and exhibit multidrug-resistant (MDR) phenotype both *in vitro* and *in vivo* [23]. We rationalized that a combination of doxorubicin and PDT using methylene blue, which can also inhibit doxorubicin efflux, will improve the accumulation of doxorubicin in tumor cells. However, for optimum efficacy, the two drugs need to be simultaneously localized in the tumor tissue. Encapsulation of the two drugs in a carrier like nanoparticles could enable their synchronized delivery to tumor cells.

In a series of studies [18,19,22], we have reported the fabrication, characterization and cellular drug delivery applications of AOT-alginate nanoparticles. Our studies show that AOT-alginate nanopar-ticles efficiently encapsulate weakly basic, polar molecules like methylene blue and doxorubicin [18]. Our proposed model for AOT-alginate nanoparticles – drug-loaded, calcium-crosslinked alginate core, surrounded by one or more bilayers composed of AOT – suggests that only the negative charges present in the core of the nanoparticle matrix (carboxyl groups in alginate) are involved in electrostatic interactions with weakly basic drug molecules. Thus, negative charges (sulfonate of AOT) on the surface of nanoparticles contribute to the negative zeta potential of drug-loaded AOT-alginate nanoparticles. Previous *in vitro* release studies show that nanoparticles release 60–70% of the encapsulated drug over 4 weeks, with near zero-order release during the first 15 days. Further mechanistic studies demonstrated that calcium–sodium exchange between nanoparticle matrix and release medium and electrostatic interaction between drug and nanoparticle matrix are important determinants of drug release.

In previous *in vitro* studies, we observed that encapsulation in AOT-alginate nanoparticles significantly enhanced the cytotoxicity of methylene blue and doxorubicin in drug-sensitive cells [19,22] and methylene blue–doxorubicin combination therapy in MDR tumor cells [25]. Nanoparticle-mediated combination therapy resulted in a significant induction of both apoptosis and necrosis in drug-resistant tumor cells. Improvement in cytotoxicity was correlated with enhanced intracellular and nuclear delivery of the two drugs. Further, nanoparticle-mediated combination therapy resulted in significantly elevated reactive oxygen species (ROS) production compared to single drug treatment. Those *in vitro* studies indicated that encapsulation of methylene blue and doxorubicin in AOT-alginate nanopar-ticles could overcome tumor drug resistance, and provided the basis for the current *in vivo* studies.

Encapsulation in nanoparticles can increase the overall accumulation of the two drugs in tumor *in vivo* through enhanced permeation and retention effect [15]. In the current study, AOT-alginate nanoparticles significantly enhanced tumor levels of doxorubicin and methylene blue compared to the free drug treatments. Incorporation in nanoparticles reduced the accumulation of doxorubicin in the heart to some extent, which could help decrease doxorubicin-associated cardiac toxicity. Cardiac toxicity limits the use of the drug in the clinic [27]. Encapsulation in nanoparticles also resulted in lower levels of methylene blue in the blood compared to the free drug treatment. Previous studies reported that upon systemic administration, methylene blue accumulates extensively in erythrocytes and blood vessel endothelial cells, where it is rapidly inactivated [14,17,28]. Improved tumor accumulation and reduced non-specific distribution could have contributed to the enhanced tumor growth inhibition observed with the combination therapy in nanoparticles. It is important to mention

that further biodistribution studies at several time-points are required to confirm the enhanced accumulation of nanoparticle-encapsulated drugs in the tumor.

The results of our studies demonstrate the importance of combining PDT with chemotherapy as well as the importance of encapsulating the combination in nanoparticles to achieve maximum inhibition of tumor growth. The marginal inhibition of tumor growth observed with methylene blue–doxorubicin nanoparticle combination in the absence of light indicated that methylene blue enhanced the efficacy of doxorubicin through other mechanisms in addition to the photody-namic effect. Methylene blue-mediated P-gp inhibition [9,29] could have resulted in increased penetration of doxorubicin into the tumor cell, resulting in enhanced inhibition of tumor growth in the dark control group [25].

Effective inhibition of tumor growth with doxorubicin has been linked to extensive induction of apoptosis [30] and some necrosis [31]. Light-activated photosensitizers also result in cell kill through apoptosis and/or necrosis [32]. Tumors treated with nanoparticle-encapsulated doxorubicin and methylene blue along with light exposure had significantly more number of apoptotic cells than those in other treatment groups. We also found significant apoptosis in tumors treated with nanoparticle-encapsulated doxorubicin and methylene blue but without light exposure. On the other hand, treatment with combination of free doxorubicin and methylene blue along with light exposure did not result in significant number of $TUNEL^+$ cells. This might be because treatment with free drugs resulted in lower concentrations of doxorubicin and methylene blue in the tumor (25 and 40% of the corresponding levels in the nanoparticle treatment group, respectively).

In addition to induction of apoptosis, effective anticancer therapy is expected to inhibit tumor cell proliferation as well [33]. PCNA is a nuclear protein synthesized in the late G_1 and S phases of the cell cycle that is used as a marker for cellular proliferation [34]. In tumors treated with combination therapy encapsulated in nanoparticles along with light exposure, there were fewer $PCNA^+$ cells compared to control groups, indicating lower levels of tumor cell proliferation. It was interesting to observe that in tumors treated with methylene blue nanoparticles, the percentage of $PCNA^+$ cells was less than that in other control groups, indicating lower levels of cell proliferation. Previous research has shown impaired tumor cell proliferation after PDT [35].

PDT can also damage tumor microvasculature, resulting in a partial shut-down of local blood supply [10,36]. CD34 staining in the combination therapy plus PDT group was diffuse and the stained vessels lacked the structural integrity observed in the other groups, indicating possible vessel damage. This does not appear to be just an effect of PDT, because other groups that received PDT, such as free doxorubicin and methylene blue followed by light exposure, did not show similar defective microvessels.

In contrast to other treatment modalities such as chemotherapy and radiotherapy, which suppress the immune system [37,38], PDT can stimulate local antitumor immune response [39]. PDT-mediated anti-tumor immunity has been linked to the recruitment of $CD8^+$ T-cells in tumor tissue [40], possibly mediated by neutrophils [41]. In addition, recent reports have indicated immune stimulation following doxorubicin treatment in a mouse tumor model [42]. Further, significant immune stimulation following PDT and low dose chemotherapy has been reported [11]. Thus, although not investigated here, combination PDT and chemotherapy could have also induced antitumor immune response, contributing to the observed tumor growth inhibition. Further studies are required to evaluate the role of antitumor immune response following combination chemotherapy and PDT.

In this study, significant tumor growth inhibition that was sustained over a 1-month period was observed with a single dose of the combination therapy nanoparticles. Multiple doses of

this treatment could provide a more significant effect and for a longer duration. However, in the mouse tumor model, performing multiple intravenous injections is technically challenging. Further, the use of cytotoxic agents like doxorubicin causes a high degree of inflammation in the fragile tail vein, which further compromises patency and limits the number of injections. For these reasons, we performed the single dose study in this model. Future studies will evaluate the feasibility of multiple dosing studies in other species.

To summarize, increased drug accumulation in the tumor and the consequent enhancement in inhibition of tumor cell proliferation and induction of apoptosis contribute to the greatly improved efficacy of nanoparticle-mediated combination chemotherapy and PDT. Damage to the tumor vasculature possibly adds to the antitumor efficacy of the combination therapy. Further, as discussed earlier, our previous studies suggest that encapsulation of methylene blue and doxorubicin in AOT-alginate nanoparticles results in significantly enhanced intracellular and nuclear accumulation of the two drugs, and in greater ROS production. Future studies will optimize treatment conditions (light dose, time of light exposure following treatment administration and repeated dosing) to further improve efficacy against drug-resistant tumors.

Acknowledgments

The funding was from the Presidential Research Enhancement Program, Wayne State University. We thank Prof. Guangzhao Mao and Dr. Hitesh Handa for assistance with AFM characterization of nanoparticles.

Abbreviations

P-gp	P-glycoprotein
PDT	photodynamic therapy
ROS	reactive oxygen species
AOT	Aerosol-OT

References

1. Mimeault M, Hauke R, Batra SK. Recent advances on the molecular mechanisms involved in the drug resistance of cancer cells and novel targeting therapies. Clin Pharmacol Ther. 2008; 83:673–691. [PubMed: 17786164]
2. Makin G, Hickman JA. Apoptosis and cancer chemotherapy. Cell Tissue Res. 2000; 301:143–152. [PubMed: 10928287]
3. Rashmi R, Kumar S, Karunagaran D. Ectopic expression of Hsp70 confers resistance and silencing its expression sensitizes human colon cancer cells to curcumin-induced apoptosis. Carcinogenesis. 2004; 25:179–187. [PubMed: 14604899]
4. Rahko E, Blanco G, Soini Y, Bloigu R, Jukkola A. A mutant TP53 gene status is associated with a poor prognosis and anthracycline-resistance in breast cancer patients. Eur J Cancer. 2003; 39:447–453. [PubMed: 12751374]
5. Szakacs G, Paterson JK, Ludwig JA, Booth-Genthe C, Gottesman MM. Targeting multidrug resistance in cancer. Nat Rev Drug Discov. 2006; 5:219–234. [PubMed: 16518375]
6. Hurwitz SJ, Terashima M, Mizunuma N, Slapak CA. Vesicular anthracycline accumulation in doxorubicin-selected U-937 cells: participation of lysosomes. Blood. 1997; 89:3745–3754. [PubMed: 9160680]
7. Alabaster O, Woods T, Ortiz-Sanchez V, Jahangeer S. Influence of microenviron-mental pH on adriamycin resistance. Cancer Res. 1989; 49:5638–5643. [PubMed: 2790781]

8. Kolarova H, Bajgar R, Tomankova K, Krestyn E, Dolezal L, Halek J. *In vitro* study of reactive oxygen species production during photodynamic therapy in ultrasound-pretreated cancer cells. Physiol Res. 2007; 56(Suppl 1):S27–S32. [PubMed: 17552898]
9. Trindade GS, Farias SL, Rumjanek VM, Capella MA. Methylene blue reverts multidrug resistance: sensitivity of multidrug resistant cells to this dye and its photodynamic action. Cancer Lett. 2000; 151:161–167. [PubMed: 10738110]
10. Fingar VH, Kik PK, Haydon PS, Cerrito PB, Tseng M, Abang E, Wieman TJ. Analysis of acute vascular damage after photodynamic therapy using benzopor-phyrin derivative (BPD). Br J Cancer. 1999; 79:1702–1708. [PubMed: 10206280]
11. Castano AP, Mroz P, Wu MX, Hamblin MR. Photodynamic therapy plus low-dose cyclophosphamide generates antitumor immunity in a mouse model. Proc Natl Acad Sci U S A. 2008; 105:5495–5500. [PubMed: 18378905]
12. Jain D. Cardiotoxicity of doxorubicin and other anthracycline derivatives. J Nucl Cardiol. 2000; 7:53–62. [PubMed: 10698235]
13. Sass MD, Caruso CJ, Axelrod DR. Accumulation of methylene blue by metabolizing erythrocytes. J Lab Clin Med. 1967; 69:447–455. [PubMed: 4381244]
14. Bongard RD, Merker MP, Shundo R, Okamoto Y, Roerig DL, Linehan JH, Dawson CA. Reduction of thiazine dyes by bovine pulmonary arterial endothelial cells in culture. Am J Physiol. 1995; 269:L78–L84. [PubMed: 7631818]
15. Iyer AK, Khaled G, Fang J, Maeda H. Exploiting the enhanced permeability and retention effect for tumor targeting. Drug Discov Today. 2006; 11:812–818. [PubMed: 16935749]
16. He XX, Wang K, Tan W, Liu B, Lin X, He C, Li D, Huang S, Li J. Bioconjugated nanoparticles for DNA protection from cleavage. J Am Chem Soc. 2003; 125:7168–7169. [PubMed: 12797777]
17. Tang W, Xu H, Park EJ, Philbert MA, Kopelman R. Encapsulation of methylene blue in polyacrylamide nanoparticle platforms protects its photodynamic effectiveness. Biochem Biophys Res Commun. 2008; 369:579–583. [PubMed: 18298950]
18. Chavanpatil MD, Khdair A, Patil Y, Handa H, Mao G, Panyam J. Polymer-surfactant nanoparticles for sustained release of water-soluble drugs. J Pharm Sci. 2007; 96:3379–3389. [PubMed: 17721942]
19. Chavanpatil MD, Khdair A, Panyam J. Surfactant-polymer nanoparticles: a novel platform for sustained and enhanced cellular delivery of water-soluble molecules. Pharm Res. 2007; 24:803–810. [PubMed: 17318416]
20. Kelly, RG.; Floyd, HA.; Jolly, ER.; Tove, PA. The pharmacokinetics and metabolism of dioctyl sodium sulfo-succinate in several animal species and man: report submitted for publication to WHO. Lederle Laboratories; American Cyanamid: 1973.
21. Shimizu T, Yamato M, Kikuchi A, Okano T. Cell sheet engineering for myocardial tissue reconstruction. Biomaterials. 2003; 24:2309–2316. [PubMed: 12699668]
22. Khdair A, Gerard B, Handa H, Mao G, Shekhar MP, Panyam J. Surfactant-polymer nanoparticles enhance the effectiveness of anticancer photodynamic therapy. Mol Pharm. 2008; 5:795–807. [PubMed: 18646775]
23. Lee BD, French KJ, Zhuang Y, Smith CD. Development of a syngeneic *in vivo* tumor model and its use in evaluating a novel P-glycoprotein modulator, PGP-4008. Oncol Res. 2003; 14:49–60. [PubMed: 14552591]
24. Orth K, Beck G, Genze F, Ruck A. Methylene blue mediated photodynamic therapy in experimental colorectal tumors in mice. J Photochem Photobiol B. 2000; 57:186–192. [PubMed: 11154085]
25. Khdair A, Handa H, Mao G, Panyam J. Nanoparticle-mediated combination chemotherapy and photodynamic therapy overcomes tumor drug resistance *in vitro*. Eur J Pharm Biopharm. 2009; 71:214–222. [PubMed: 18796331]
26. Ozben T. Mechanisms and strategies to overcome multiple drug resistance in cancer. FEBS Lett. 2006; 580:2903–2909. [PubMed: 16497299]
27. Doroshow JH. Doxorubicin-induced cardiac toxicity. N Engl J Med. 1991; 324:843–845. [PubMed: 1997858]

28. Williams JL, Stamp J, Devonshire R, Fowler GJ. Methylene blue and the photo-dynamic therapy of superficial bladder cancer. J Photochem Photobiol B. 1989; 4:229–232. [PubMed: 2512384]
29. Rumjanek VM, Trindade GS, Wagner-Souza K, de Oliveira MC, Marques-Santos LF, Maia RC, Capella MA. Multidrug resistance in tumour cells: characterization of the multidrug resistant cell line K562-Lucena 1. An Acad Bras Cienc. 2001; 73:57–69. [PubMed: 11246270]
30. Stearns V, Singh B, Tsangaris T, Crawford JG, Novielli A, Ellis MJ, Isaacs C, Pennanen M, Tibery C, Farhad A, Slack R, Hayes DF. A prospective randomized pilot study to evaluate predictors of response in serial core biopsies to single agent neoadjuvant doxorubicin or paclitaxel for patients with locally advanced breast cancer. Clin Cancer Res. 2003; 9:124–133. [PubMed: 12538460]
31. Weinberg BD, Ai H, Blanco E, Anderson JM, Gao J. Antitumor efficacy and local distribution of doxorubicin via intratumoral delivery from polymer millirods. J Biomed Mater Res A. 2007; 81:161–170. [PubMed: 17120197]
32. Wyld L, Reed MW, Brown NJ. Differential cell death response to photodynamic therapy is dependent on dose and cell type. Br J Cancer. 2001; 84:1384–1386. [PubMed: 11355951]
33. Denoyelle C, Albanese P, Uzan G, Hong L, Vannier JP, Soria J, Soria C. Molecular mechanism of the anti-cancer activity of cerivastatin, an inhibitor of HMG-CoA reductase, on aggressive human breast cancer cells. Cell Signal. 2003; 15:327–338. [PubMed: 12531431]
34. Roos G, Landberg G, Huff JP, Houghten R, Takasaki Y, Tan EM. Analysis of the epitopes of proliferating cell nuclear antigen recognized by monoclonal antibodies. Lab Invest. 1993; 68:204–210. [PubMed: 7680082]
35. Romanko YS, Tsyb AF, Kaplan MA, Popuchiev VV. Relationship between antitumor efficiency of photodynamic therapy with photoditasine and photo-energy density. Bull Exp Biol Med. 2005; 139:460–464. [PubMed: 16027881]
36. Krammer B. Vascular effects of photodynamic therapy. Anticancer Res. 2001; 21:4271–4277. [PubMed: 11908681]
37. Orlova RV, Chernetsova LF, Matveeva ON. Effect of systemic chemotherapy on clinical status and biological and immunologic markers in patients with breast cancer. Vopr Onkol. 2007; 53:414–418. [PubMed: 17969403]
38. Friedman EJ. Immune modulation by ionizing radiation and its implications for cancer immunotherapy. Curr Pharm Des. 2002; 8:1765–1780. [PubMed: 12171547]
39. Castano AP, Mroz P, Hamblin MR. Photodynamic therapy and anti-tumour immunity. Nat Rev Cancer. 2006; 6:535–545. [PubMed: 16794636]
40. Kabingu E, Vaughan L, Owczarczak B, Ramsey KD, Gollnick SO. CD8+ T cell-mediated control of distant tumours following local photodynamic therapy is independent of CD4+ T cells and dependent on natural killer cells. Br J Cancer. 2007; 96:1839–1848. [PubMed: 17505510]
41. Kousis PC, Henderson BW, Maier PG, Gollnick SO. Photodynamic therapy enhancement of antitumor immunity is regulated by neutrophils. Cancer Res. 2007; 67:10501–10510. [PubMed: 17974994]
42. Casares N, Pequignot MO, Tesniere A, Ghiringhelli F, Roux S, Chaput N, Schmitt E, Hamai A, Hervas-Stubbs S, Obeid M, Coutant F, Metivier D, Pichard E, Aucouturier P, Pierron G, Garrido C, Zitvogel L, Kroemer G. Caspase-dependent immunogenicity of doxorubicin-induced tumor cell death. J Exp Med. 2005; 202:1691–1701. [PubMed: 16365148]

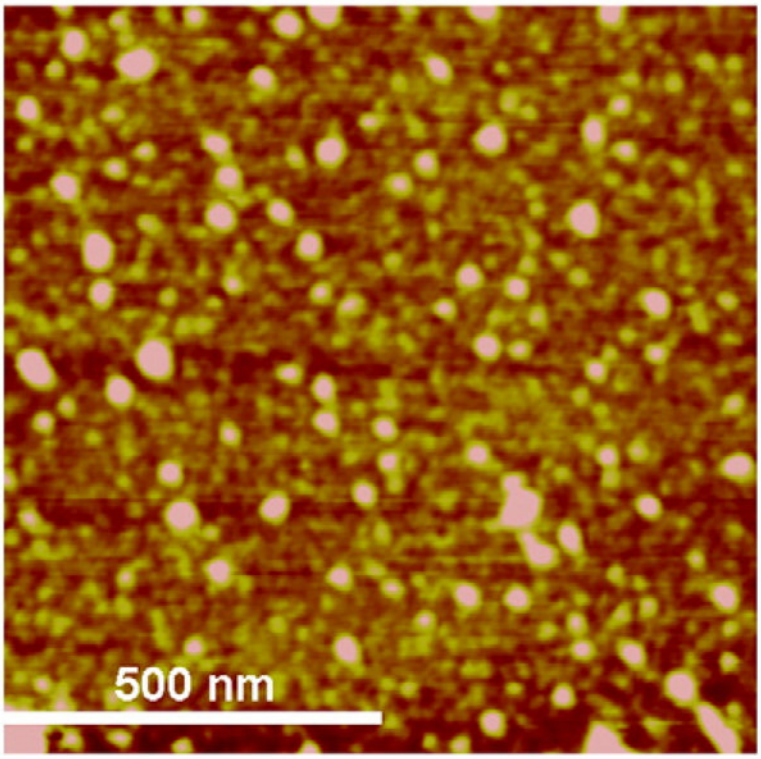

Fig. 1.
A height image of nanoparticles loaded with doxorubicin and methylene blue acquired by tapping-mode atomic force microscopy in air.

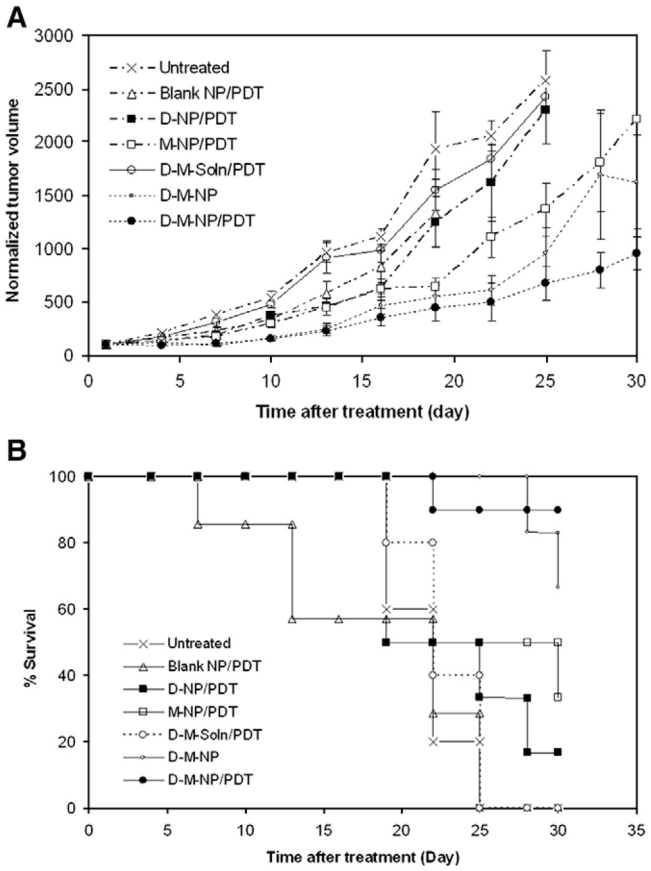

Fig. 2.

(A) Tumor growth inhibition curve and (B) Kaplan–Meier survival plot of Balb/c mice bearing subcutaneous JC tumor. Mice received empty nanoparticles plus light exposure (Blank NP/PDT), methylene blue nanoparticles plus light exposure (M-NP/PDT), doxorubicin nanoparticles plus light exposure (D-NP/PDT), nanoparticles loaded with doxorubicin and methylene blue without light exposure (D-M-NP), nanoparticles loaded with methylene blue and doxorubicin plus light exposure (D-M-NP/PDT), doxorubicin and methylene blue in solution plus light exposure (D-M-soln/PDT), or just the vehicle plus light exposure (vehicle). Tumors were measured and animal survival were monitored every 3rd day until day 30 or tumor volume ≥2000 mm^3. Data as mean±SD (n=7–10 mice).

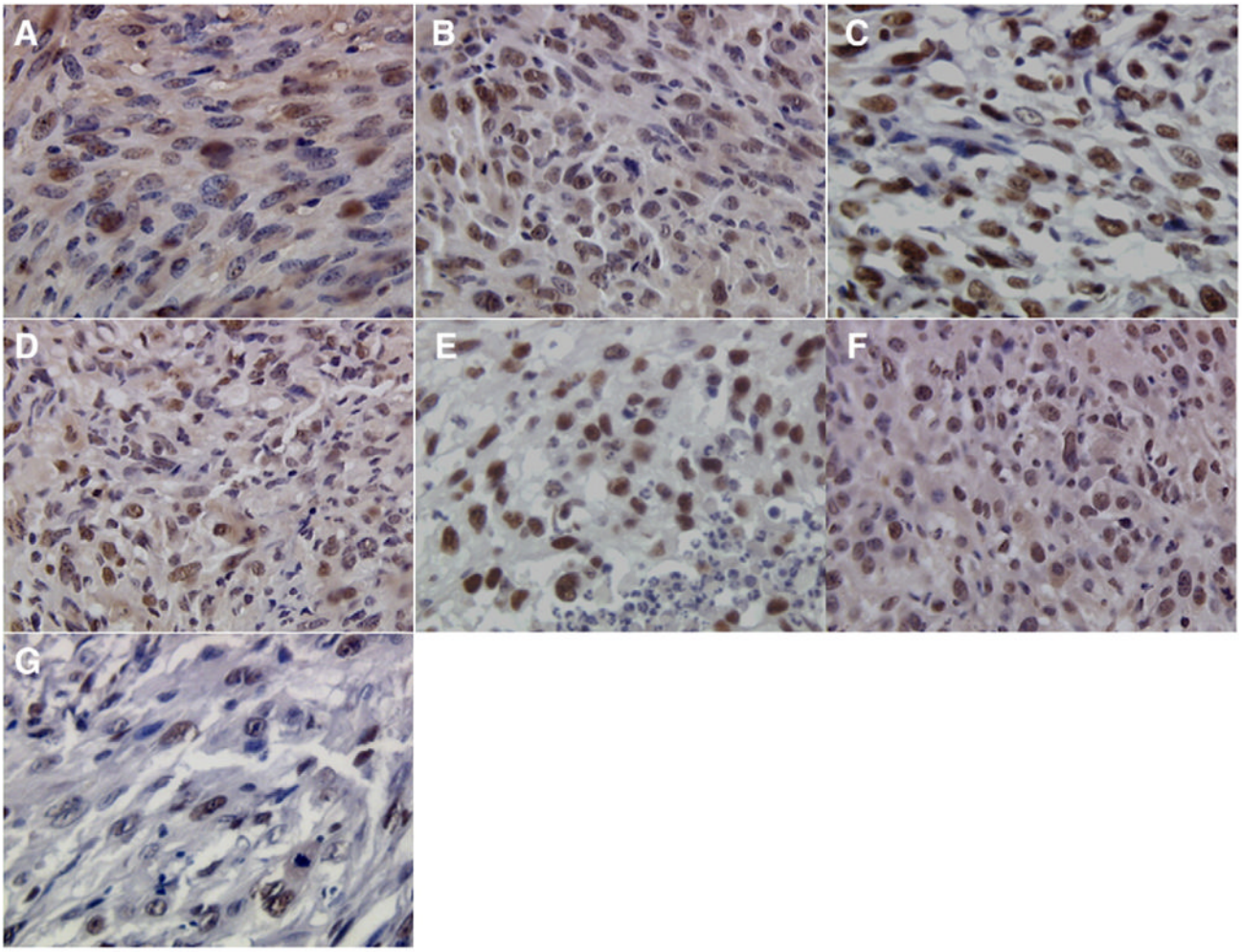

Fig. 3.
PCNA staining of sections from tumors that received (A) vehicle plus light exposure, (B) blank nanoparticles plus light exposure, (C) doxorubicin nanoparticles plus light exposure, (D) methylene blue nanoparticles plus light exposure, (E) doxorubicin and methylene blue in solution plus light exposure, (F) nanoparticles loaded with doxorubicin and methylene blue without light exposure, and (G) nanoparticles loaded with methylene blue and doxorubicin plus light exposure. Images were acquired at 400× magnification.

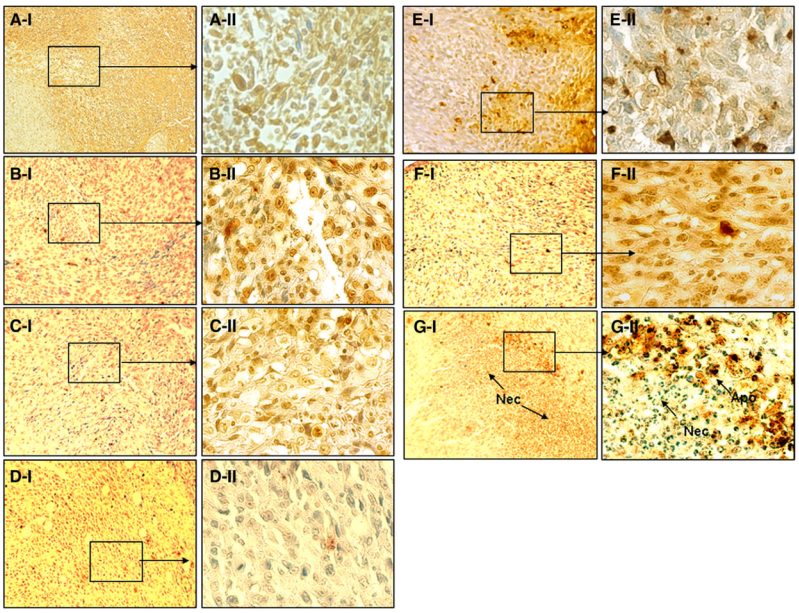

Fig. 4.

TUNEL staining for different treatment groups: vehicle plus light exposure (A), blank nanoparticles plus light exposure (B), doxorubicin nanoparticles plus light exposure (C), methylene blue nanoparticles plus light exposure (D), doxorubicin and methylene blue in solution plus light exposure (E), nanoparticles loaded with doxorubicin and methylene blue without light exposure (F), and nanoparticles loaded with methylene blue and doxorubicin plus light exposure (G). Sections were imaged at 100× (I) or 400× (II).

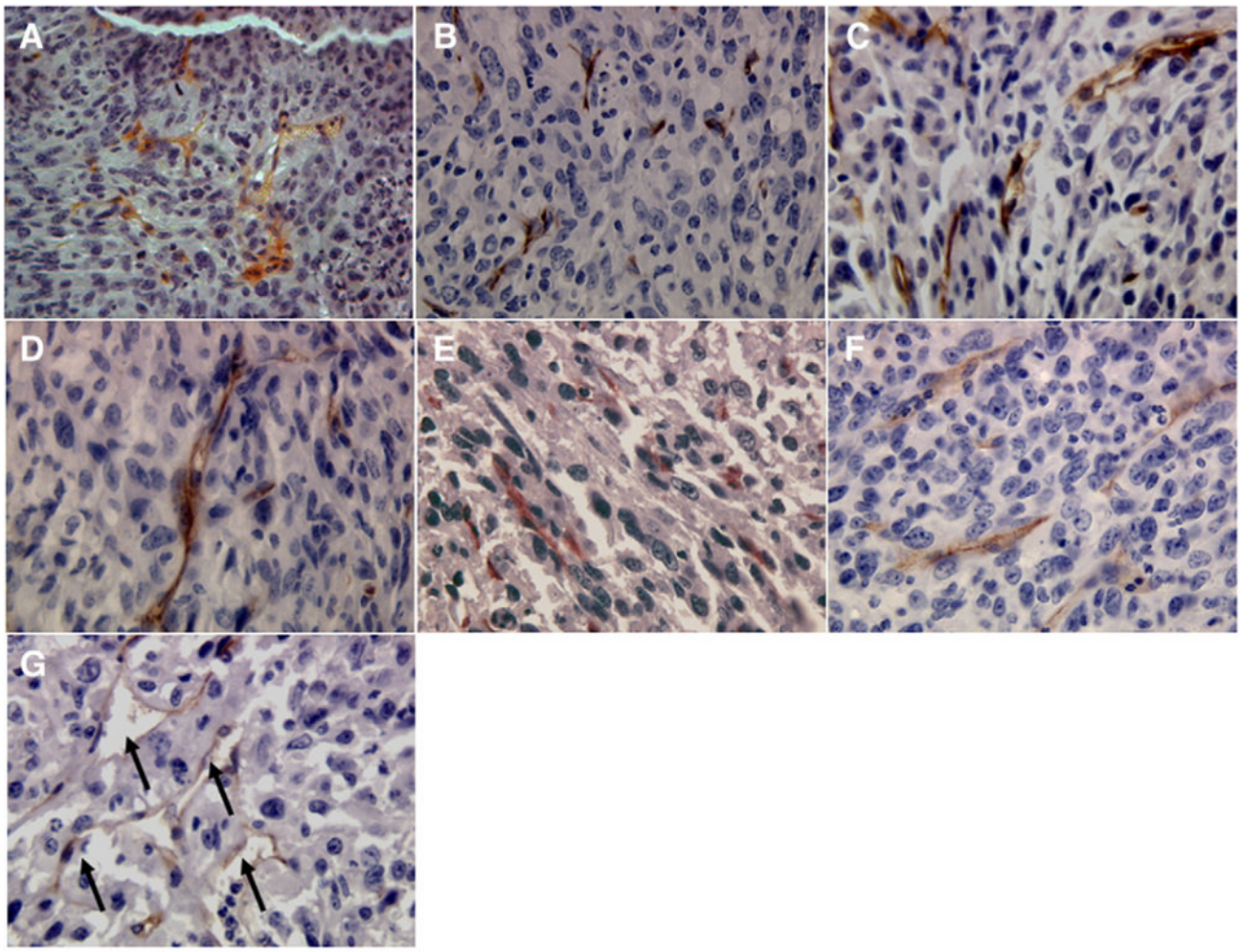

Fig. 5.

CD34 staining of sections from tumors that received (A) vehicle plus light exposure, (B) blank nanoparticles plus light exposure, (C) doxorubicin nanoparticles plus light exposure, (D) methylene blue nanoparticles plus light exposure, (E) doxorubicin and methylene blue in solution plus light exposure, (F) nanoparticles loaded with doxorubicin and methylene blue without light exposure, and (G) nanoparticles loaded with methylene blue and doxorubicin plus light exposure. Images were acquired at 400× magnification.

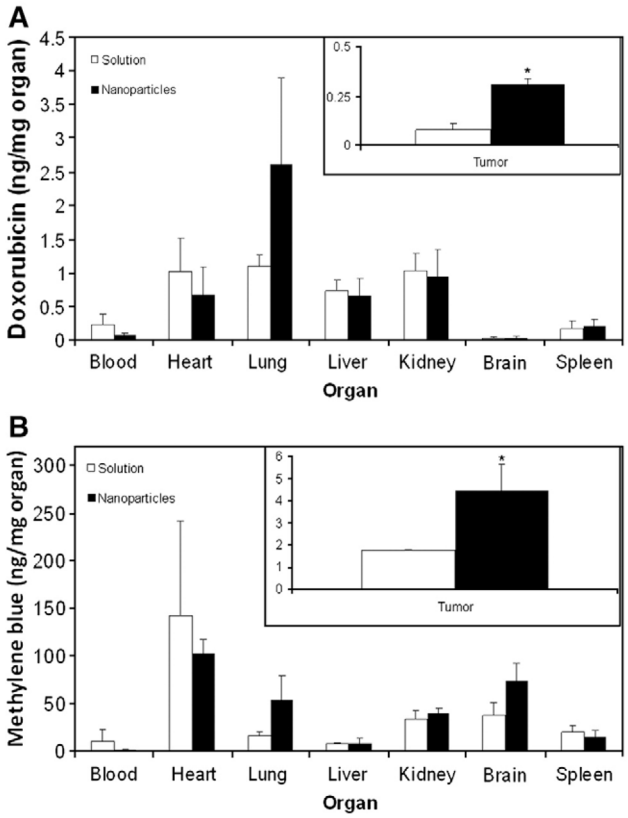

Fig. 6.

Effect of encapsulation in nanoparticles on the biodistribution of (A) doxorubicin and (B) methylene blue. Balb/c mice bearing subcutaneous JC tumor were intravenously injected with a combination of doxorubicin and methylene blue either free in solution or encapsulated in nanoparticles. Animals were euthanized 3 h after treatment administration and tumors were collected. Doxorubicin and methylene blue concentrations in tumors and other organs were determined using LC-MS/MS and normalized to the dry organ weight. Data as mean±SD (n=3–4). *p<0.05, t-test.